

Enhanced nonlinear response of superconductor-normal-conductor composite wires and strips

Wing-Hon Siu and K. W. Yu

Department of Physics, The Chinese University of Hong Kong, Shatin, New Territories, Hong Kong

(Received 29 August 1995; revised manuscript received 17 October 1995)

The effective response is calculated in nonlinear composite wires and strips which are modeled as two-dimensional random conductance networks with lateral size L and width $\delta \ll L$. We consider a two-component nonlinear conductance network which consists of two types of conductors. The first component is assumed to be nonlinear and obeys a current-voltage (I - V) characteristic of the form $I = \sigma_1 V + \chi_1 V^3$, while the second component is linear with $I = \sigma_2 V$, where σ_1 and σ_2 are the linear conductances and χ_1 is the nonlinear conductance. We invoke a renormalization-group (RG) analysis to rescale the strip repeatedly by small-cell transformations to obtain a chain of nonlinear conductors, for which *exact* formulas of the effective linear response σ_e and nonlinear response χ_e are available. We calculate σ_e and χ_e as a function of the volume fraction for various conductance ratios and examine the dependence on δ . We observe large enhancements in the nonlinear response under appropriate conditions, as well as interesting crossover from one- to two-dimensional behaviors as δ increases. Numerical simulations are performed to verify the RG calculations. Scaling exponents are determined in the RG and compared with available estimates; good agreements are found. Possible generalizations of the present investigation are discussed.

I. INTRODUCTION

The physics of nonlinear inhomogeneous media has been a subject of considerable current interest because of their potential applications in engineering and science.¹⁻⁶ In particular, much effort has been centered around the calculations of the effective response in nonlinear composite systems consisting of two or more materials of different dielectric functions or conductivities.^{1,7-13} In the weakly nonlinear regime in which the nonlinearity can be treated as a small perturbation, various methods have been established.⁷⁻⁹ Recently much effort has been devoted to strongly nonlinear composites.¹⁰⁻¹³

It is observed that the effective response of composite media can differ to a large extent from that of their constituents.¹ The widely varying constitutive properties lead to large variations in the local electric fields and currents and, hence, to large enhancements or decreases in the effective properties. Such an enhancement effect may be more pronounced in nonlinear composites.¹⁴ It has been shown that the effective nonlinear response can be enormously enhanced near the percolation threshold under appropriate conditions.¹⁵ Recently, large enhancements in the effective nonlinear response have also been found in fractal clustering in nonlinear composites.¹⁶ It is therefore believed, from the above considerations, that the effective nonlinear response may depend strongly on geometry-controlled properties, e.g., the dimensionality of the composite systems.

Recently, significant advances have been made in materials fabrication techniques. By means of molecular-beam epitaxial techniques, samples of various materials with desired geometry, size, interface, and surface conditions are available and they show profound potential in applications. Hence geometry-controlled properties have become one of the important areas to explore, both theoretically and practically. We have also seen the technological importance of composite thin films and nanowires. In this work, we use a simple

nonlinear conductance network model to study the effective nonlinear responses of composite wires and strips, in which the lateral size is much larger than the width. We shall use a renormalization-group (RG) analysis to calculate the effective linear and nonlinear responses. We find large enhancements in the effective nonlinear response under certain conditions, and more interestingly, we find a crossover from one- to two-dimensional behaviors as the width increases. Numerical simulations are performed to verify the RG calculations.

The paper is organized as follows. In the next section, we present a formalism for weakly nonlinear composites and reiterate the established formulas for the effective linear and nonlinear responses. In Sec. III, we derive exact formulas for the effective linear and nonlinear responses of composite wires. In Sec. IV, we use the RG analysis to deal with composite strips of finite width. We shall perform numerical simulation to verify the RG calculations. In Sec. V, we discuss the scaling behaviors of the effective responses and determine the scaling exponents in the RG and compared with available estimates. Possible generalizations of the present work will be discussed.

II. FORMALISM

Consider a d -dimensional (dD), two-component hypercubic nonlinear conductance network which consists of two types of conductors. The first component is assumed to be nonlinear and obeys a current-voltage (I - V) characteristic of the form

$$I = \sigma_1 V + \chi_1 V^3, \quad (1)$$

where σ_1 and χ_1 are the linear and nonlinear conductance, respectively. Throughout this work, the nonlinearity is assumed to be weak so that $\chi_1 V^2 / \sigma_1 \ll 1$ and we restrict ourselves to cubic nonlinearity. This form of nonlinearity, usually called "Kerr-like," is common in materials with

inversion symmetry and has received extensive study. The second component is assumed linear with

$$I = \sigma_2 V, \quad (2)$$

where σ_2 is the linear conductance. The volume fractions of the first and second components are p and q , respectively, and $p+q=1$. We are interested in calculating the effective linear and nonlinear responses of the network, represented by a homogeneous network of identical conductors, each of which has an I - V characteristic of the form

$$I = \sigma_e V + \chi_e V^3, \quad (3)$$

where σ_e and χ_e are the effective linear and nonlinear responses, respectively, and are given by the voltage-summation formulas^{8,9,15}

$$\sigma_e = \frac{1}{\Omega} \sum_{\alpha} \sigma_{\alpha} V_{\alpha}^2, \quad (4)$$

$$\chi_e = \frac{1}{\Omega} \sum_{\alpha} \chi_{\alpha} V_{\alpha}^4, \quad (5)$$

where σ_{α} and χ_{α} are the linear and nonlinear responses of the α th conductor; $\Omega = \prod_{i=1}^d L_i$, where L_i is the lateral size along the i th Cartesian coordinate. Without loss of generality, we apply a voltage along the x_1 direction and open boundary conditions in the remaining $(d-1)$ directions. We have also adopted the convention that the voltage across the two opposite $(d-1)$ -dimensional hyperplanes is L_1 . In Eqs. (4) and (5), V_{α} is the voltage difference across the α th conductor in the *linear* random problem (i.e., obtained by solving the same random network problem with all $\chi_{\alpha}=0$). The summation is performed over all conductors in the network.

In what follows, we shall consider a two-dimensional (2D) rectangular strip of length $L_1=L$ and width $L_2=\delta$, with $\delta \ll L$. We shall calculate σ_e and χ_e and examine their dependence on width δ . Interesting crossover from one- to two-dimensional behaviors will be observed.

III. LINEAR AND NONLINEAR RESPONSES OF COMPOSITE WIRES

We first examine the $\delta=1$ case; i.e., we have a chain of nonlinear conductors. Consider a chain of L conductors, k of which are of type 1 (σ_1, χ_1), while the remaining $(L-k)$ of which are of type 2 (σ_2, χ_2), subject to an applied voltage $V=L$ along the chain. For convenience, we denote the conductance ratio $h = \sigma_2/\sigma_1$. By using the circuit formula for series combination of linear conductances, we obtain the voltages $V_1 = hL/(L-k+hk)$ and $V_2 = L/(L-k+hk)$ across type 1 and 2 conductors, respectively. By using the voltage-summation formulas (4) and (5), together with simple combinatorial considerations, we arrive at the *exact* formulas for the effective linear and nonlinear responses of a composite wire:

$$\sigma_e = \sum_{k=0}^L \binom{L}{k} p^k q^{L-k} \frac{L\sigma_1\sigma_2}{(L-k)\sigma_1 + k\sigma_2} \quad (6)$$

and

$$\chi_e = \sum_{k=0}^L \binom{L}{k} p^k q^{L-k} \frac{L^3[\chi_1 k h^4 + \chi_2(L-k)]}{(L-k+hk)^4}. \quad (7)$$

Two important limits are worth studying: (1) the normal conductor-insulator (N/I) case in which the second component is poorer conducting ($h \ll 1$) and (2) the superconductor-normal-conductor (S/N) case in which the second component is better conducting ($h \gg 1$). For simplicity and without loss of generality, we take $\chi_2=0$; i.e., the second component is always linear. The wire formulas can be used to calculate σ_e and χ_e for both cases. For the N/I case, we find a large decrease in the effective nonlinear response while a large enhancement occurs for the S/N case. We shall present results for the S/N case (Fig. 1) for illustration. The length of wire $L=32$. In Fig. 1, we plot the normalized effective linear response (σ_e/σ_1) and nonlinear response (χ_e/χ_1) as a function of the volume fraction p for various conductance ratio $h>1$. We observe a large enhancement in the effective nonlinear response χ_e . The enhancement increases with the conductance ratio while the locations of maximum response of χ_e occur at $p^* \approx 1/L$, a result independent of h . The location of peak p^* can be calculated numerically from Eq. (7) in the limit of large h . We find $p^* = 0.268, 0.135, 0.067, 0.034, \text{ and } 0.017$ for $L=4, 8, 16, 32, \text{ and } 64$, respectively. The result is in reasonable agreement with the numerical calculations presented in Fig. 1 for $L=32$. For clarity, in the insets of Fig. 1, we also show the normalized linear and nonlinear responses in a semilogarithmic plot.

We are now in a position to extract the critical behavior of the effective linear and nonlinear responses of a chain near percolation. In the limit $L \rightarrow \infty$, we find $V_1 = h/(q+ph)$ and $V_2 = 1/(q+ph)$ across type 1 and 2 conductors, respectively. Again, by using the voltage-summation formulas, we find $\sigma_e = \sigma_1 h/(q+ph)$ and $\chi_e = \chi_1 p h^4/(q+ph)^4$, respectively. In the S/N limit, i.e., $h \rightarrow \infty$, we find $\sigma_e \rightarrow \sigma_1(1-q)^{-1}$ and $\chi_e \rightarrow \chi_1(1-q)^{-3}$. If we write $\sigma_e \approx \sigma_1(q_c - q)^{-s}$ and $\chi_e \approx \chi_1(q_c - q)^{-w}$, we identify the superconducting exponent $s=1$ and the nonlinear exponent $w=3$. Hence we should observe a large enhancement in the effective nonlinear response near the percolation threshold of the second component; we find $q_c=1$.

Moreover, for a large but finite ratio h , and near percolation, we find $\sigma_e = \sigma_1(q_c - q)^{-1}F(z)$ and $\chi_e = \chi_1(q_c - q)^{-3}G(z)$, where $F(z) = (1+z)^{-1}$ and $G(z) = (1+z)^{-4}$ are scaling functions of the variable $z = h^{-1}(q_c - q)^{-1}$. Hence we identify the crossover exponent $\phi=1$. If we write $\phi = s+t$, we find the conductivity exponent $t=0$ in one dimension.¹⁷ For a large but finite L , we expect the percolation correlation length diverges as $\xi_p \approx L \approx 1/p = (q_c - q)^{-1}$. Hence we identify the percolation correlation length exponent $\nu=1$ in one dimension.¹⁷ In this regard, we may propose finite-size scaling forms for σ_e and χ_e : $\sigma_e = \sigma_1 L f(h^{-1}L)$ and $\chi_e = \chi_1 L^3 g(h^{-1}L)$, where f and g are finite-size scaling functions.

IV. LINEAR AND NONLINEAR RESPONSES OF COMPOSITE STRIPS

When interwire couplings are present, we may model the system by a nonlinear composite strip of a finite width δ . For

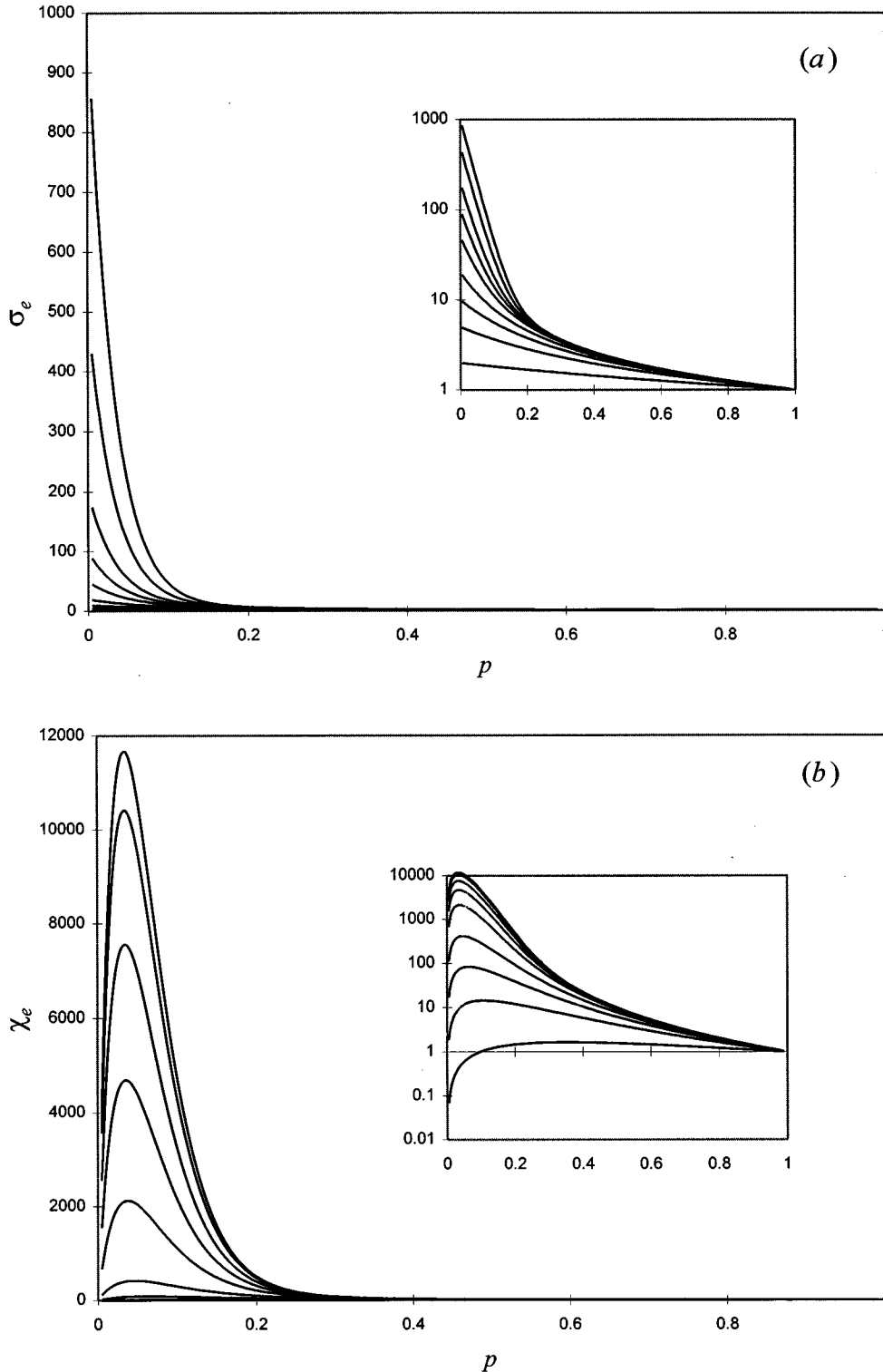


FIG. 1. For $L=32$ composite wires, the normalized effective (a) linear response (σ_e/σ_1) and (b) nonlinear response (χ_e/χ_1) are plotted as a function of the volume fraction p for various conductance ratio h in the S/N limit. We observe a large enhancement in the effective nonlinear response χ_e , which increases with h while the location of maximum nonlinear response occurs at $p^* \approx 1/L$, roughly independent of h . For clarity, in the insets we show σ_e/σ_1 and χ_e/χ_1 in a semilogarithmic plot. From bottom to top in order of increasing conductance ratio, $h=2, 5, 10, 20, 50, 100, 200, 500$, and 1000 .

$\delta=2$, we have a ladder network. Exact analytic results can only be obtained for $h=\sigma_2/\sigma_1=0$.¹⁷ Unfortunately, for a finite conductance ratio h , we are unable to solve the composite strip problem exactly. We resort to a renormalization-group (RG) analysis^{18–20} because we believe that the RG approximation is able to capture local field fluctuations better than the effective medium approximation. The idea of RG is to rescale the strip repeatedly by a simple small-cell trans-

formation, to obtain a wire of a shorter length. In this way, we obtain a set of renormalized parameters $p', q', \sigma'_1, \sigma'_2, \chi'_1$, and χ'_2 ; $h'=\sigma'_2/\sigma'_1$. The RG analysis goes with the following steps. We start out with a strip of dimension $L \times \delta$, at a conductance ratio $h=\sigma_2/\sigma_1$ and probability p . The nonlinear bonds have a finite χ_1 and $\chi_2=0$. However, one should note that although we start out with a linear second component, the renormalized one will gener-

ally be nonlinear, i.e., $\chi'_2 \neq 0$. We perform an approximate 2×2 cell RG calculation to reduce the dimension of the strip to $(L/2) \times (\delta/2)$.

Consider a 2×2 cell, identical with a $L=2$, $\delta=2$ ladder with five conductors, each of which is of type 1 (σ_1, χ_1) and type 2 (σ_2, χ_2) with probability p and q , respectively. It is easy to see that there is only one configuration with all five bonds superconducting (probability q^5), five superconducting configurations with four bonds superconducting and one bond normal conducting (probability $5p^4q$), eight superconducting configurations with three bonds superconducting and two bonds normal conducting (probability $8p^3q^2$), and two superconducting configurations with two bonds superconducting and three bonds normal conducting (probability $2p^2q^3$). Hence the entire 2×2 cell is superconducting with a probability q' given by¹⁸⁻²⁰

$$q' = R_2(q) = 2p^3q^2 + 8p^2q^3 + 5p^4q + q^5. \quad (8)$$

A similar analysis can be performed for the nonsuperconducting configurations; we find $p' = 1 - q'$.

Accordingly, we divide the $2^5 = 32$ possible configurations into two sets, one of which is superconducting (i.e., the second component is spanning the cell), while the other of which is nonspanning. If we apply a voltage $V=2$ across the cell, we can calculate the linear voltages across the 5 bonds of each of the 32 configurations. The voltage-summation formulas can be used to evaluate the effective linear and nonlinear response of a given configuration. We then perform certain averages over the 16 spanning configurations to obtain σ'_2 and χ'_2 , while over the remaining 16 nonspanning configurations to obtain σ'_1 and χ'_1 . We obtain the following results:

$$\begin{aligned} \sigma'_1 &= \Phi_1(\sigma_1, \sigma_2, p) \\ &= \exp \left[\frac{1}{R_2(p)} \left(p^5 \ln \sigma_1 + p^4 q \ln \sigma_1 + 2p^3 q^2 \ln \frac{2\sigma_1 \sigma_2}{\sigma_1 + \sigma_2} + 2p^2 q^3 \ln \frac{2\sigma_1 \sigma_2}{\sigma_1 + \sigma_2} + 2p^3 q^2 \ln \frac{\sigma_1(\sigma_1 + 3\sigma_2)}{3\sigma_1 + \sigma_2} \right. \right. \\ &\quad \left. \left. + 4p^4 q \ln \frac{\sigma_1(3\sigma_1 + 5\sigma_2)}{5\sigma_1 + 3\sigma_2} + 4p^3 q^2 \ln \frac{\sigma_1(\sigma_1^2 + 5\sigma_1 \sigma_2 + 2\sigma_2^2)}{2\sigma_1^2 + 5\sigma_1 \sigma_2 + \sigma_2^2} \right) \right], \end{aligned} \quad (9)$$

$$\begin{aligned} \sigma'_2 &= \Phi_2(\sigma_1, \sigma_2, p) \\ &= \exp \left[\frac{1}{R_2(q)} \left(p q^4 \ln \sigma_2 + q^5 \ln \sigma_2 + 2p^3 q^2 \ln \frac{\sigma_1 + \sigma_2}{2} + 2p^2 q^3 \ln \frac{\sigma_1 + \sigma_2}{2} + 2p^2 q^3 \ln \frac{\sigma_2(3\sigma_1 + \sigma_2)}{\sigma_1 + 3\sigma_2} \right. \right. \\ &\quad \left. \left. + 4p q^4 \ln \frac{\sigma_2(5\sigma_1 + 3\sigma_2)}{3\sigma_1 + 5\sigma_2} + 4p^2 q^3 \ln \frac{\sigma_2(2\sigma_1^2 + 5\sigma_1 \sigma_2 + \sigma_2^2)}{\sigma_1^2 + 5\sigma_1 \sigma_2 + 2\sigma_2^2} \right) \right], \end{aligned} \quad (10)$$

$$\begin{aligned} \chi'_1 &= \Psi_1(\chi_1, \chi_2, h, p) \\ &= 4 \exp \left[\frac{1}{R_2(p)} \left(p^5 \ln \frac{\chi_1}{4} + p^4 q \ln \frac{\chi_1}{4} + 2p^3 q^2 \ln \frac{2(\chi_2 + \chi_1 h^4)}{(1+h)^4} + 2p^2 q^3 \ln \frac{2(\chi_2 + \chi_1 h^4)}{(1+h)^4} \right. \right. \\ &\quad \left. \left. + 2p^3 q^2 \ln \frac{3\chi_1 + 32\chi_2 + 4\chi_1 h + 18\chi_1 h^2 + 4\chi_1 h^3 + 3\chi_1 h^4}{(3+h)^4} \right. \right. \\ &\quad \left. \left. + 4p^4 q \ln \frac{99\chi_1 + 256\chi_2 + 180\chi_1 h + 210\chi_1 h^2 + 180\chi_1 h^3 + 99\chi_1 h^4}{(5+3h)^4} \right. \right. \\ &\quad \left. \left. + 4p^3 q^2 \ln \frac{2\chi_1 + 17\chi_2 + 20\chi_1 h + \dots + 82\chi_1 h^6 + 20\chi_1 h^7 + 2\chi_1 h^8}{(2+5h+h^2)^4} \right) \right], \end{aligned} \quad (11)$$

$$\begin{aligned} \chi'_2 &= \Psi_2(\chi_1, \chi_2, h, p) \\ &= 4 \exp \left[\frac{1}{R_2(q)} \left(p q^4 \ln \frac{\chi_2}{4} + q^5 \ln \frac{\chi_2}{4} + 2p^3 q^2 \ln \frac{\chi_1 + \chi_2}{8} + 2p^2 q^3 \ln \frac{\chi_1 + \chi_2}{8} \right. \right. \\ &\quad \left. \left. + 2p^2 q^3 \ln \frac{3\chi_2 + 4\chi_2 h + 18\chi_2 h^2 + 4\chi_2 h^3 + 32\chi_1 h^4 + 3\chi_2 h^4}{(1+3h)^4} \right. \right. \\ &\quad \left. \left. + 4p q^4 \ln \frac{99\chi_2 + 180\chi_2 h + 210\chi_2 h^2 + 180\chi_2 h^3 + 256\chi_1 h^4 + 99\chi_2 h^4}{(3+5h)^4} \right. \right. \\ &\quad \left. \left. + 4p^2 q^3 \ln \frac{2\chi_2 + 20\chi_2 h + 82\chi_2 h^2 + \dots + 20\chi_2 h^7 + 17\chi_1 h^8 + 2\chi_2 h^8}{(1+5h+2h^2)^4} \right) \right], \end{aligned} \quad (12)$$

and $h' = \Phi(h, p) = \Phi_2(1, h, p) / \Phi_1(1, h, p)$, where Φ , Φ_1 , Φ_2 , Ψ_1 , and Ψ_2 are transformations of their arguments. In obtaining Eqs. (9)–(12), we have invoked a geometrical mean over spanning and nonspanning configurations¹⁹ while Eqs. (11) and (12) represent a generalization of the established RG analysis^{18–20} to the nonlinear response. We prefer the geometric mean because it gives results better compared with simulation data to be considered in the following. More importantly, the geometric mean is able to satisfy duality symmetry in 2D random conductance networks.¹⁹ We then repeat the RG several times until $\delta' = 1$. Of course, for a $\delta = 2$ ladder, one RG has already done so, while for a $\delta = 4$ strip, two consecutive RG's are needed. We end up with a composite wire of a shorter length L' , with renormalized quantities p' , σ'_1 , σ'_2 , h' , χ'_1 , and χ'_2 . The wire formulas [Eqs. (6) and (7)] can therefore be used to obtain the effective linear and nonlinear responses of composite strips.

It is instructive to obtain the critical behavior of the RG transformations near percolation. Equation (8) possesses three fixed points $q^* = 0, \frac{1}{2},$ and 1 , with $q^* = q_c = \frac{1}{2}$ being an unstable fixed point, to be identified with the percolation threshold of the second component. From the fixed-point analysis at q_c , we find the inverse of the percolation correlation length exponent $1/\nu = \log_2(13/8) \approx 0.70$, to be compared with the *exact* value $1/\nu = 0.75$ in two dimensions. Right at the percolation threshold $q = q_c$ (or $p = p_c$) and in the limit $h \rightarrow \infty$, one finds $\sigma'_1 \approx 1.843\sigma_1$, while $\chi'_1 \approx 5.738\chi_1$. Hence we find the superconducting exponent $s \approx 1.26$, to be compared with $s = 1.297$ from numerical simulation.¹⁷ We also find the nonlinear exponent $w = 3.60$, to be compared with $w = 3.71$ from available estimates on noise exponents.²¹ Moreover, right at q_c and in the limit of large $h = \sigma_2/\sigma_1$, we find $h' = \sigma'_2/\sigma'_1 \approx 0.2943h$ from Eqs. (9) and (10). Hence we determine the crossover exponent $\phi/\nu = \log_2(1/0.2943) \approx 1.76$, to be compared with the established value $\phi/\nu = 1.949$ from numerical simulation.¹⁷ We also find that $s/\nu \approx 0.88$, to be compared with $s/\nu = 0.9745$ from numerical simulation,¹⁷ while $w/\nu \approx 2.52$, to be compared with $w/\nu = 2.79$ from available estimates.²¹ Again, if we write $\phi = s + t$, we find the conductivity exponent $t/\nu \approx 0.88$. Hence the RG analysis explicitly satisfies duality symmetry in two dimensions.

In what follows, we restrict ourselves to the S/N case only and present RG results for $\delta = 2$ ladders and for $\delta = 4$ strips. Again, we take $L = 32$ and $\chi_2 = 0$ for comparison with the wire results in the previous section. We first present numerical RG results for a $\delta = 2$ ladder. In Fig. 2, we plot σ_e/σ_1 and χ_e/χ_1 as a function of the volume fraction p for various conductance ratios h . Again, we observe a large enhancement in the effective nonlinear response. The enhancement increases with the conductance ratio while the location of maximum response of χ_e has shifted to a larger p^* , an estimate of which will be discussed below. However, it is also noted that the strength of enhancement has decreased slightly.

We then present numerical RG results for a $\delta = 4$ strip. In Fig. 3, we plot σ_e/σ_1 and χ_e/χ_1 as a function of the volume fraction p for various conductance ratios h . Similarly, we

observe a large enhancement in the effective nonlinear response. The enhancement increases with the conductance ratio while the location of maximum response of χ_e has now shifted to an even larger p^* , indicating a crossover from 1D to 2D behaviors. It is also noted that the strength of enhancement has decreased substantially as compared to the small- δ cases. This is attributed to the large fluctuations of local electric fields present at small δ , leading to a large enhancement in the nonlinear response.

To establish a result for the location of peak, we invoke the RG analysis. The shift of p^* towards the 2D value as δ increases is attributed to the fact that the renormalized wire length decreases with δ . By using Eq. (8), we obtain for $32 \times \delta$ strips, $p^* = 0.034, 0.175, 0.336,$ and 0.443 for $\delta = 1, 2, 4,$ and 8 , respectively, values that are in good agreement with the numerical calculations presented in Figs. 2 and 3. These values can be interpreted as the effective percolation threshold of a strip of finite width.^{20,21} It is evident that the peak of response shifts towards the 2D percolation threshold $p_c = 0.5$ as δ increases. Incidentally, the present RG analysis gives the exact p_c in 2D. Hence a clear crossover from 1D to 2D behavior has been observed.

To confirm the RG result, we perform numerical simulations in nonlinear conductance networks. We have done simulations for 32×2 and 32×4 networks. Details of the numerical simulations can be found in Ref. 15. We present results for the S/N case only. In the insets of Figs. 2 and 3, we also show the normalized effective linear and nonlinear responses of numerical simulation in a semilogarithmic plot for comparison. As evident from the figures, a reasonable agreement between the RG and simulation data is obtained. The agreement is even better for large ratios. In this connection, it is tempting to fit the simulation data by a simple effective medium approximation⁷ (EMA) but parametrized by $p_c \approx p^*$. It has been found that while the EMA fits the simulation data of σ_e reasonably well, strongly deviations are nevertheless observed for the effective nonlinear response χ_e . This is attributed to the fact that the EMA ignores local field fluctuations explicitly.

V. SCALING BEHAVIORS

In this section, we shall study the scaling behaviors of the effective linear and nonlinear responses of composite strips of arbitrary lengths and widths. For strips of infinite length $L \rightarrow \infty$, we may apply the scaling theory of Neimark²² to obtain the effective percolation threshold $q_c(\delta)$ of a finite width δ ,

$$q_c(\delta) = q_c^{2D} + (q_c^{1D} - q_c^{2D})\delta^{-1/\nu_{2D}}, \quad (13)$$

where $q_c^{1D} = 1$ and $q_c^{2D} = 1/2$ are the percolation thresholds in one and two dimensions, respectively, and ν_{2D} is the percolation correlation length exponent in 2D. By using the exact values for $\nu_{2D} = 4/3$, we can calculate $q_c(\delta)$ and hence $p_c(\delta)$. We find $p_c(\delta) = 0.203, 0.323, 0.395,$ and 0.438 for $\delta = 2, 4, 8,$ and 16 , respectively. If we use the RG estimate for $\nu = 1/0.70$, we find $p_c(\delta) = 0.192, 0.311, 0.383,$ and 0.428 for $\delta = 2, 4, 8,$ and 16 , respectively, values that are slightly smaller. However, these values are in qualitative

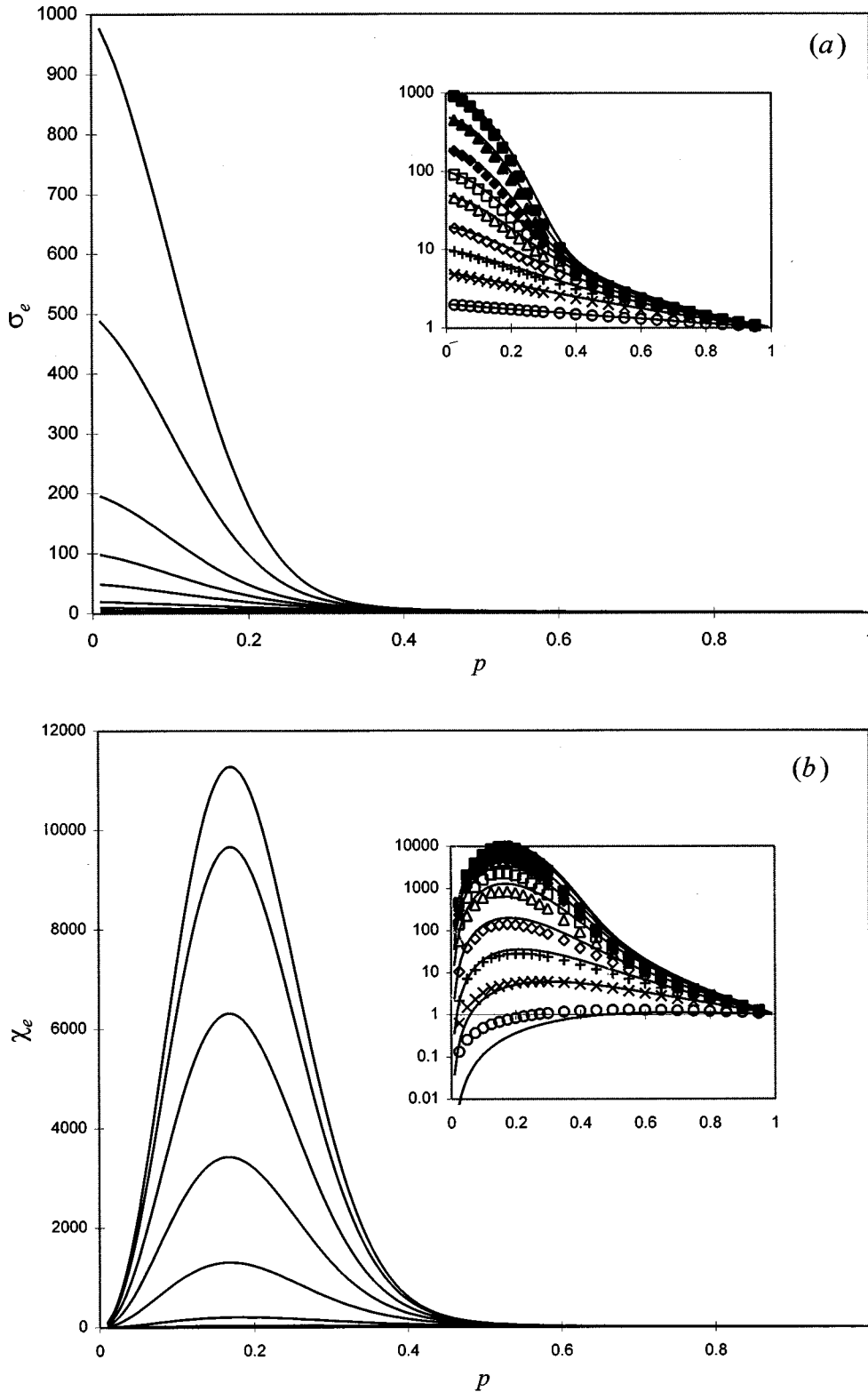


FIG. 2. For $\delta=2$ ladder and $L=32$, the (a) linear response σ_e/σ_1 and (b) nonlinear response χ_e/χ_1 are plotted as a function of the volume fraction p for various h . Again, we observe a large enhancement in χ_e . The location of maximum nonlinear response has shifted to a larger p^* , the value of which coincides with the estimate of RG analysis. It is also noted that the strength of enhancement has decreased slightly. In the insets, we show the numerical simulation (symbols) in a semilogarithmic plot. From bottom to top in order of increasing conductance ratio, $h=2, 5, 10, 20, 50, 100, 200, 500$, and 1000 . As evident from the figures, a reasonable agreement between the RG and simulation data is obtained. The agreement is even better for large h .

agreement with the RG estimates of p^* for strips of $L=32$, presented in the previous section.

For strips of finite length, however, there are three variables to be considered, namely, the finite length L , width δ , and ratio h of conductances. Forming scaling variables

among these three variables, we construct universal scaling functions of two variables.¹⁷ By rescaling our RG and numerical data appropriately, it may be possible to collapse data onto one single universal curve. In what follows, we shall limit ourselves to $q=q^*$ (or $p=p^*$), $h=\infty$, and

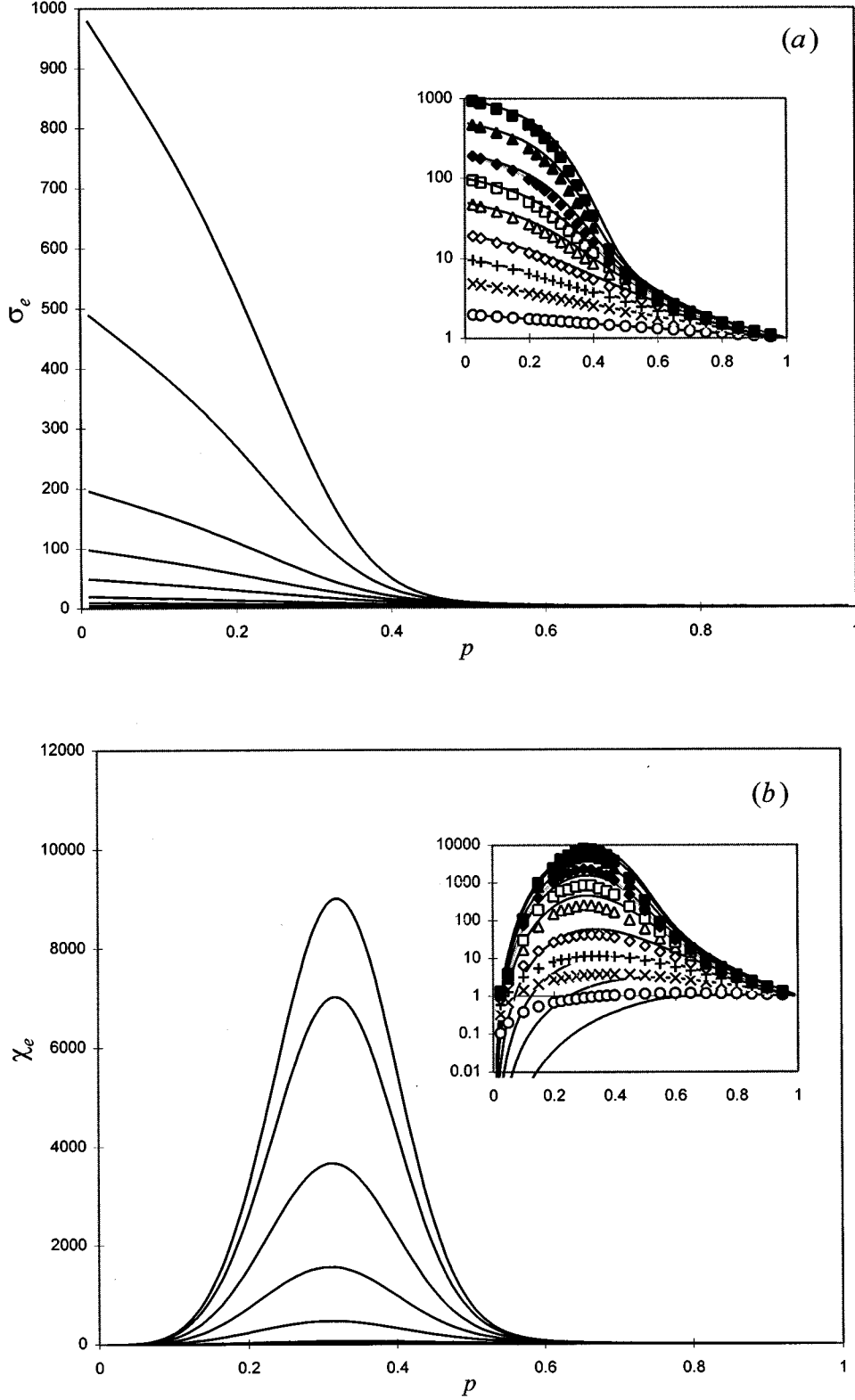


FIG. 3. Similar to Fig. 2, but for a $\delta=4$ strip. We observe a large enhancement in χ_e . The location of maximum response of χ_e has now shifted to an even larger p^* , indicating a crossover from 1D to 2D behaviors. It is also noted that the strength of enhancement has decreased substantially. In the insets, we also show the simulation data (symbols). As evident from the figures, a reasonable agreement between the RG and simulation data is obtained.

$\delta \ll L$. For strips of finite length L , we propose the following scaling forms for σ_e and χ_e in analogy with the scaling theory of Neimark,²² pertaining to a two- to three-dimensional crossover:

$$\sigma_e \approx \sigma_1 \delta^{-(s_{1D}/\nu_{1D} - s_{2D}/\nu_{2D})} L^{s_{1D}/\nu_{1D}}, \quad (14)$$

$$\chi_e \approx \chi_1 \delta^{-(w_{1D}/\nu_{1D} - w_{2D}/\nu_{2D})} L^{w_{1D}/\nu_{1D}}, \quad (15)$$

where we have explicitly distinguished exponents in one and two dimensions. One can readily show that for a fixed width δ and $L \rightarrow \infty$, $\sigma_e \approx \sigma_1 L^{s_{1D}/\nu_{1D}}$, and one recovers the one-dimensional behavior, while for $\delta \rightarrow L$, $\sigma_e \approx \sigma_1 L^{s_{2D}/\nu_{2D}}$, and

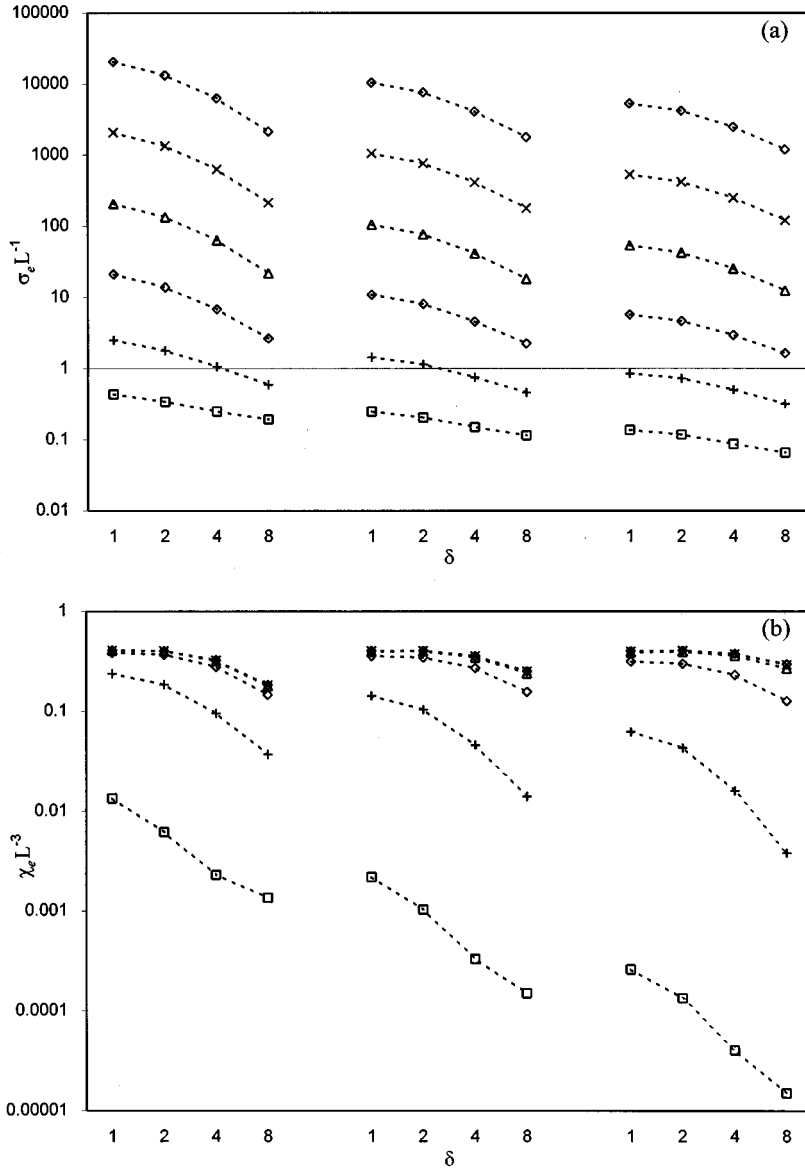


FIG. 4. For various length of strips, the rescaled effective linear and nonlinear responses (a) $\sigma_e/\sigma_1 L$ and (b) $\chi_e/\chi_1 L^3$ are plotted as a function of the width δ for various ratio h in a log-log plot. The data are displaced into three separate groups: left ($L=16$), middle ($L=32$), and right ($L=64$). The width δ ranges from 1 to 8. From bottom to top in order of increasing ratios, $h=10, 10^2, 10^3, 10^4, 10^5$, and 10^6 . The lines are only guides to the eyes. It is evident from the plot that as h increases, the rescaled nonlinear response converges rapidly to the $h=\infty$ limit. The gradual decrease of the rescaled response σ_e and χ_e with increasing δ is evident from the plots, in qualitative agreement with the asymptotic scaling relations.

one recovers the two-dimensional behavior. The same conclusions can be drawn for χ_e . Using the numerical values of the critical exponents from Secs. III and IV, we find generally $s_{1D}/\nu_{1D} > s_{2D}/\nu_{2D}$ and $w_{1D}/\nu_{1D} > w_{2D}/\nu_{2D}$, valid both for the RG analysis and available estimates. Hence a gradual decrease in the enhanced nonlinear response is evident as the width δ becomes large. We find $s_{1D}/\nu_{1D} - s_{2D}/\nu_{2D} \approx 0.12$ in RG and 0.026 in numerical simulations, respectively, while $w_{1D}/\nu_{1D} - w_{2D}/\nu_{2D} \approx 0.48$ in RG and 0.21 in numerical simulations, respectively.

To verify the scaling relations, we plot in Fig. 4 the rescaled effective linear and nonlinear responses $\sigma_e/\sigma_1 L$ and $\chi_e/\chi_1 L^3$ as a function of the width δ in a log-log plot for various ratios and for various length and width of strips. The data are displaced into three separate groups along the δ axis: left ($L=16$), middle ($L=32$), and right ($L=64$). For the effective linear response, we observe a gradual decrease of the rescaled response $\sigma_e/\sigma_1 L$ as δ increases, in qualitative agreement with the asymptotic scaling relation [Eq. (14)]. Moreover, the results agree among the three sets of L values. For the effective nonlinear response, it is evident

from the plots that as h increases, the rescaled nonlinear responses $\chi_e/\chi_1 L^3$ converge rapidly to the $h=\infty$ limits. In this regard, if one had used only nonspanning configurations to calculate σ_e , the effective linear response would have shown saturation too. The gradual decrease of the rescaled nonlinear response with increasing δ is evident from the plot, in qualitative agreement with the asymptotic scaling relations [Eq. (15)]. Hence the scaling forms are verified.

VI. DISCUSSIONS AND CONCLUSIONS

Here a few comments on the results are in order. Although the discussion has been limited to couplings within the plane only, an extension can be readily made to realistic composite systems in three dimensions (3D). We expect that similar results can be obtained, namely, a large enhancement of the effective nonlinear response under appropriate conditions and a crossover from 1D to 3D behaviors can be observed. The enhancement as well as dimensionality crossover effects may possibly be observed in experiments on electrorheological (ER) systems where an inherent nonlinear characteristic

occurs due to the formation of columnar structures in the ER systems under the application of intense electric fields.²³

Moreover, generalization can also be made to thin composite films²⁴ of metallic particles embedded in dielectric host, in which case δ plays the role of the thickness of the film and a crossover from 2D to 3D behaviors can be observed. Possible experiments may also be done on the optical properties of nonlinear composite thin films. In this connection, a simple EMA is shown to give a reasonable fit of the simulation data²⁴ in linear composite thin films. However, we believe that the present RG analysis may fit the effective nonlinear response better. In order to test the asymptotic scaling theory,²² pertaining to the 2D to 3D dimensionality crossover, extensive simulation as well as RG analysis should be performed. Relevant studies include the extraction of the effective percolation threshold, critical exponents, and universal scaling functions.¹⁵ The work should be left for future studies.^{25,26}

In summary, the effective response has been calculated in nonlinear composite wires and strips with lateral size L much larger than the width δ . We have used the renormalization-group analysis to calculate the effective linear and nonlinear responses as a function of the volume fraction p for various conductance ratio h and examine their dependence on δ . We observe large enhancements in the nonlinear response under appropriate conditions, as well as interesting crossover from 1D to 2D behaviors as δ increases. Numerical simulations are performed and compared well with the RG calculations.

ACKNOWLEDGMENTS

This work was supported by the Research Grants Council of the Hong Kong Government under Project Nos. CUHK 78/93E and 461/95P. We thank Professor D. Stroud for sending us a copy of his work²⁴ prior to publication.

-
- ¹D. J. Bergman and D. Stroud, in *Solid State Physics*, edited by H. Ehrenreich and D. Turnbull (Academic, New York, 1992), Vol. 46, p. 147.
- ²See the articles in *Proceedings of the Third International Conference on Electrical Transport and Optical Properties in Inhomogeneous Media* [Physica A **207**, 1 (1994)].
- ³See the articles in *Breakdown and Nonlinearity in Soft Condensed Matter*, edited by K. K. Bardhan, B. K. Chakrabarti, and A. Hansen, Springer Lecture Notes in Physics (Springer, New York, 1994).
- ⁴See the articles in J. Opt. Soc. Am. B **6**, No. 4 (1989); C. Flytzanis, Prog. Opt. **29**, 2539 (1992).
- ⁵J. W. Haus, R. Inguva, and C. M. Bowden, Phys. Rev. A **40**, 5729 (1990); M. J. Bloemer, P. R. Ashley, J. W. Haus, N. Kalyaniwalla, and C. R. Christensen, IEEE J. Quantum Electron. **QE-26**, 1075 (1990).
- ⁶D. Stroud and V. E. Wood, J. Opt. Soc. Am. B **6**, 778 (1989); A. E. Neeves and M. H. Birnboim, *ibid.* **6**, 787 (1989); Y. Q. Li, C. C. Sung, R. Inguva, and C. M. Bowden, *ibid.* **6**, 814 (1989).
- ⁷D. Stroud and P. M. Hui, Phys. Rev. B **37**, 8719 (1988); X. C. Zeng, D. J. Bergman, P. M. Hui, and D. Stroud, *ibid.* **38**, 10 970 (1988).
- ⁸G. Q. Gu and K. W. Yu, Phys. Rev. B **46**, 4502 (1992); K. W. Yu and G. Q. Gu, *ibid.* **47**, 7568 (1993).
- ⁹K. W. Yu, Y. C. Wang, P. M. Hui, and G. Q. Gu, Phys. Rev. B **47**, 1782 (1993); K. W. Yu, P. M. Hui, and D. Stroud, *ibid.* **47**, 14 150 (1993).
- ¹⁰R. Blumenfeld and D. J. Bergman, Phys. Rev. B **44**, 7378 (1991).
- ¹¹P. Ponte Castaneda, J. Mech. Phys. Solids **39**, 45 (1991); P. Ponte Castaneda, G. deBotton, and G. Li, Phys. Rev. B **46**, 4387 (1992).
- ¹²K. W. Yu and G. Q. Gu, Phys. Lett. A **193**, 311 (1994).
- ¹³H. C. Lee and K. W. Yu, Phys. Lett. A **197**, 341 (1995); H. C. Lee, W. H. Siu, and K. W. Yu, Phys. Rev. B **52**, 4217 (1995).
- ¹⁴X. Zhang and D. Stroud, Phys. Rev. B **49**, 944 (1994).
- ¹⁵K. W. Yu and P. M. Hui, Phys. Rev. B **50**, 13 327 (1994).
- ¹⁶K. W. Yu, E. M. Y. Chan, Y. C. Chu, and G. Q. Gu, Phys. Rev. B **51**, 11 416 (1995); K. W. Yu, *ibid.* **49**, 9989 (1994).
- ¹⁷J. P. Clerc, G. Giraud, M. Laugier, and J. M. Luck, Adv. Phys. **39**, 191 (1990).
- ¹⁸P. J. Reynolds, W. Klein, and H. E. Stanley, J. Phys. C **10**, L167 (1977).
- ¹⁹J. Bernasconi, Phys. Rev. B **18**, 2185 (1978).
- ²⁰For a more recent description of the renormalization-group method, see D. Stauffer and A. Aharony, *Introduction to Percolation Theory*, 2nd ed. (Taylor & Francis, London, 1992).
- ²¹R. Rammal, C. Tannous, and A.-M. S. Tremblay, Phys. Rev. A **31**, 2662 (1985); R. Rammal, C. Tannous, P. Breton, and A.-M. S. Tremblay, Phys. Rev. Lett. **54**, 1718 (1985).
- ²²A. V. Neimark, Zh. Éksp. Teor. Fiz. **98**, 611 [Sov. Phys. JETP **71**, 341 (1990)].
- ²³See the articles in *Fourth International Conference on Electrorheological (ER) Fluids* [Int. J. Mod. Phys. B **8**, 2721 (1994)].
- ²⁴X. Zhang and D. Stroud, Phys. Rev. B **52**, 2131 (1995).
- ²⁵P. M. Hui, W. M. V. Wan, and K. H. Chung, Phys. Rev. B **52**, 15 867 (1995). These authors have studied the dimensional crossover of the effective nonlinear response in thin films.
- ²⁶W. H. Siu and K. W. Ju. J. Phys.: Condens. Matter **8**, 419 (1996); and (unpublished). These authors have applied the RG method to study the crossover from one- to three-dimensional behaviors in composite wires and developed a renormalized effective medium approximation for thin films.